

Research Article
Periodontal Science



Bone regeneration and biosorption patterns of different bone substitutes: an *in vivo* study in rabbit skulls

Seunghee Lee ¹, Jungwoo Jung ¹, Jungwon Lee ^{1,2,*}, Young-Chang Ko ¹, Dongseob Lee ^{1,3}, Ki-Tae Koo ¹, Yang-Jo Seol ¹, Yong-Moo Lee ^{1,*}

¹Department of Periodontology and Dental Research Institute, School of Dentistry, Seoul National University, Seoul, Korea

²One-Stop Specialty Center, Seoul National University Dental Hospital, Seoul, Korea

³National Dental Care Center for Persons with Special Needs, Seoul National University Dental Hospital, Seoul, Korea



Received: Jul 6, 2024

Accepted: Oct 21, 2024

Published online: Dec 9, 2024

*Correspondence:

Jungwon Lee

Department of Periodontology and Dental Research Institute, School of Dentistry, Seoul National University, 101 Daehak-ro, Jongno-gu, Seoul 03080, Korea.

Email: houy1980@snu.ac.kr

Tel: +82-2-6256-3318

Fax: +82-2-744-0051

Yong-Moo Lee

Department of Periodontology and Dental Research Institute, School of Dentistry, Seoul National University, 101 Daehak-ro, Jongno-gu, Seoul 03080, Korea.

Email: ymlee@snu.ac.kr

Tel: +82-2-6256-3148

Fax: +82-2-744-0051

Copyright © 2025. Korean Academy of Periodontology

This is an Open Access article distributed under the terms of the Creative Commons Attribution Non-Commercial License (<https://creativecommons.org/licenses/by-nc/4.0/>).

ORCID iDs

Seunghee Lee

<https://orcid.org/0009-0009-4567-3982>

Jungwoo Jung

<https://orcid.org/0009-0002-7851-4936>

Jungwon Lee

<https://orcid.org/0000-0002-5508-442X>

Young-Chang Ko

<https://orcid.org/0009-0006-1766-6740>

ABSTRACT

Purpose: This study aimed to analyze the bone regeneration and biosorption patterns of different bone substitutes in a rabbit skull defect model.

Methods: Four circular 8 mm-defects were created in the cranium of 12 New Zealand white rabbits, each weighing approximately 3 kg. Each defect was randomly assigned to one of 4 treatment groups: cortical deproteinized porcine bone mineral (DPBM), cancellous DPBM, biphasic calcium phosphate (BCP) with a 6:4 ratio of hydroxyapatite (HA) to β -tricalcium phosphate (β -TCP) (TCP4), and BCP with a 2:8 ratio of HA to β -TCP (TCP8). The rabbits were euthanized at either 6 weeks (n=6) or 12 weeks (n=6) post-surgery. The harvested specimens were then analyzed both radiographically and histomorphometrically.

Results: In the micro-computed tomography analysis, no statistically significant differences were observed among the 4 groups, except in the bone graft volume/tissue volume (GV/TV) at 12 weeks. Cortical DBPM exhibited a higher GV/TV ratio than cancellous DBPM at the same time point. The histomorphometric analysis revealed increased biosorption in cancellous DBPM compared to cortical DBPM at 12 weeks. However, the percentage of newly formed bone did not significantly differ among the 4 groups.

Conclusions: All types of bone substitutes demonstrated similar patterns of bone regeneration at both 6 and 12 weeks of observation. However, cancellous DPBM exhibited a higher rate of bioabsorption compared to other bone substitutes, suggesting that it may have different indications or applications in guided bone regeneration protocols.

Keywords: Biocompatible materials; Bone regeneration; Bone substitutes; Skull; Membranes; X-ray microtomography

INTRODUCTION

Autogenous bone graft has long been considered the gold standard for bone regeneration, prized for its biological properties of osteoconduction, osteoinduction, and osteogenesis [1]. However, the harvesting of autogenous bone can present several drawbacks in clinical settings, including being time-consuming, increasing patient morbidity, and leading to postoperative complications [2,3]. Additionally, clinicians may face challenges due to limited

Dongseob Lee 

<https://orcid.org/0000-0003-4146-3119>

Ki-Tae Koo 

<https://orcid.org/0000-0002-9809-2630>

Yang-Jo Seol 

<https://orcid.org/0000-0002-2076-5452>

Yong-Moo Lee 

<https://orcid.org/0000-0002-5619-3847>

Funding

This study was sponsored by Purgo Biologics (Seongnam, Korea) and a grant from the National Research Foundation of Korea (No. 2022R1F1A1067588), Daejeon, Republic of Korea.

Conflict of Interest

The authors have stated that there are no conflicts of interest with regard to this study. The grant was partially provided by Purgo Biologics (Seongnam, Korea). However, the company did not provide any role in the design of the study; the collection, analysis, and interpretation of data; the writing of the manuscript; or the decision to publish the results.

Author Contributions

Conceptualization: Yong Moo Lee; Data curation: Seunghee Lee; Formal analysis: Young Chang Ko, Dongseob Lee, Ki Tae Koo, Yang Jo Seol, Yong Moo Lee; Investigation: Seunghee Lee, Jungwoo Jung; Methodology: Yong Moo Lee; Project administration: Jungwon Lee; Software: Seunghee Lee; Supervision: Yong Moo Lee, Jungwon Lee; Validation: Seunghee Lee; Writing - original draft: Seunghee Lee, Jungwoo Jung; Writing - review & editing: Young Chang Ko, Dongseob Lee, Ki Tae Koo, Yang Jo Seol, Yong Moo Lee, Jungwon Lee.

bone quantity and unpredictable bone quality [4]. Consequently, there has been a growing need for bone substitutes. In response, allografts, xenografts, and a variety of synthetic alloplasts, including hydroxyapatite (HA) and β -tricalcium phosphate (β -TCP), have been extensively studied as alternatives to autogenous bone graft.

Xenografts, including deproteinized bovine bone matrix (DBBM), are the most commonly used materials in clinical settings, supported by extensive preclinical and clinical data over many years [5,6]. Although DBBM has been widely utilized in clinical surgical procedures, deproteinized porcine bone matrix (DPBM) has emerged as an alternative xenograft material, demonstrating significant success in bone regeneration compared to DBBM [7-9]. Additionally, cancellous DPBM has shown structural, porosity, and microstructural crystallite characteristics similar to those of human cancellous bone. It also facilitates the formation of interconnected porous networks, thereby increasing the void space available for new bone graft material [10,11]. Furthermore, DPBM shows higher levels of hydrophilicity and surface energy, which promote protein adsorption, cell adhesion, and proliferation processes compared to DBBM. These properties suggest that DPBM may be more suitable for bone grafts than DBBM [8].

Meanwhile, it has been reported that cortical and cancellous autografts exhibit different bone healing patterns [12,13]. In cancellous autografts, the bone healing process occurs through creeping substitution, which involves a phase of appositional bone formation followed by a resorptive phase. Conversely, in cortical autografts, healing is achieved through reverse creeping substitution, where initial osteoclastic activity must precede osteoblastic activity and subsequent new bone formation. Interestingly, the integration of autograft with host bone typically completes around 6 months after the bone graft procedure and is usually concluded by 12 months. However, cortical autografts may still be present even 12 months post-procedure [14]. However, these biological characteristics have not been thoroughly investigated in DPBM, necessitating further *in vivo* studies.

Biphasic calcium phosphate (BCP), an alloplastic bone substitute composed of HA and β -TCP, has been effectively used in bone graft procedures [15-17]. HA not only up-regulates osteogenic genes such as ALP, COL1, and OCN in pluripotent stem cells but also stabilizes the augmented bone area [18,19]. β -TCP provides space for new bone formation by being replaced by host bone [18,19]. A higher HA ratio contributes to volume stability but may also limit space for *de novo* bone formation due to its stability and insolubility [20]. Conversely, a higher β -TCP ratio can lead to a greater amount of vital bone formation, although it may also result in a higher resorption rate of the bone substitutes [21]. Therefore, the HA: β -TCP ratio plays a crucial role in determining the BCP's capacity for bone formation [22]. The 6:4 HA: β -TCP ratio in BCP has been the most widely used in bone graft procedures and is reported to be highly predictable [23,24]. Meanwhile, other studies have investigated different ratios (2:8), demonstrating significant effects on new bone formation and serving as optimal scaffolds for stem-cell-induced bone formation [25]. However, the optimal ratio for HA: β -TCP has not yet been determined.

A systematic review and meta-analysis examined the histomorphometric analysis of allografts, xenografts, and alloplasts for alveolar ridge preservation, revealing no significant differences among the various bone graft materials [26]. However, there is still a lack of comprehensive research comparing porcine-derived xenografts with alloplasts that have varying HA/ β -TCP ratios in terms of bone regeneration. Therefore, this study aimed to

analyze the patterns of bone regeneration and biosorption in cancellous DPBM, cortical DPBM, and BCP (HA:β-TCP=6:4 and HA:β-TCP=2:8) using a rabbit skull defect model.

MATERIALS AND METHODS

Animals

Twelve white New Zealand rabbits, each weighing approximately 3 kg and aged 9–20 months, were utilized in this study. Each animal was housed in a separate cage and maintained under standard conditions: a temperature of 22°C, humidity controlled at 60%, and a 12:12-hour light-dark cycle, consistent with previous studies [27,28]. They had *ad libitum* access to water and a standard pellet food diet. The rabbits' weight was measured before and after the experiment. If more than 15% of the baseline weight was lost during the follow-up period, the data were not reflected in the experimental results. The preparation protocol was approved by the Seoul National University Animal Research Committee (SNU-230823-5-1). The animal procedures were performed in the animal laboratory at Seoul National University Graduate School of Dentistry.

Sample size calculation

In this study, the number of animals was determined based on the mean difference of $\geq 10\%$ and a standard deviation of 5.5% for this study with an alpha of 0.05 and a statistical power of 80%. To calculate the sample size, we used a software program (G*Power, Heinrich Heine University, Düsseldorf, Germany) and our previous study [27]. Inter-animal variability was assessed through power analysis, considering factors such as age, weight and sex to minimize variation. A total of 12 animals were selected, taking into account the 2 observation periods of 6 weeks and 12 weeks.

Assignment to experimental groups

Each surgically created defect was randomly assigned to one of 4 experimental groups, based on the surgical protocol using 4 different bone substitutes (**Figure 1**) as follows:

Group A (cancellous DPBM): Deproteinized porcine bone mineral derived from cancellous bone (THE Graft, Purgo Biologics, Seongnam, Korea) covered with an absorbable collagen membrane (THE Cover, Purgo Biologics).

Group B (cortical DPBM): Deproteinized porcine bone mineral derived from cortical bone (THE Graft Cortical, Purgo Biologics) covered with an absorbable collagen membrane (THE Cover, Purgo Biologics).

Group C (TCP4): Biphasic calcium phosphate with a HA:β-TCP ratio of 6:4 (THE BCP, Purgo Biologics) covered with an absorbable collagen membrane (THE Cover, Purgo Biologics).

Group D (TCP8): Biphasic calcium phosphate with a HA:β-TCP ratio of 2:8 (MBCP, Biomatlante, Nantes, France) covered with an absorbable collagen membrane (THE Cover, Purgo Biologics).

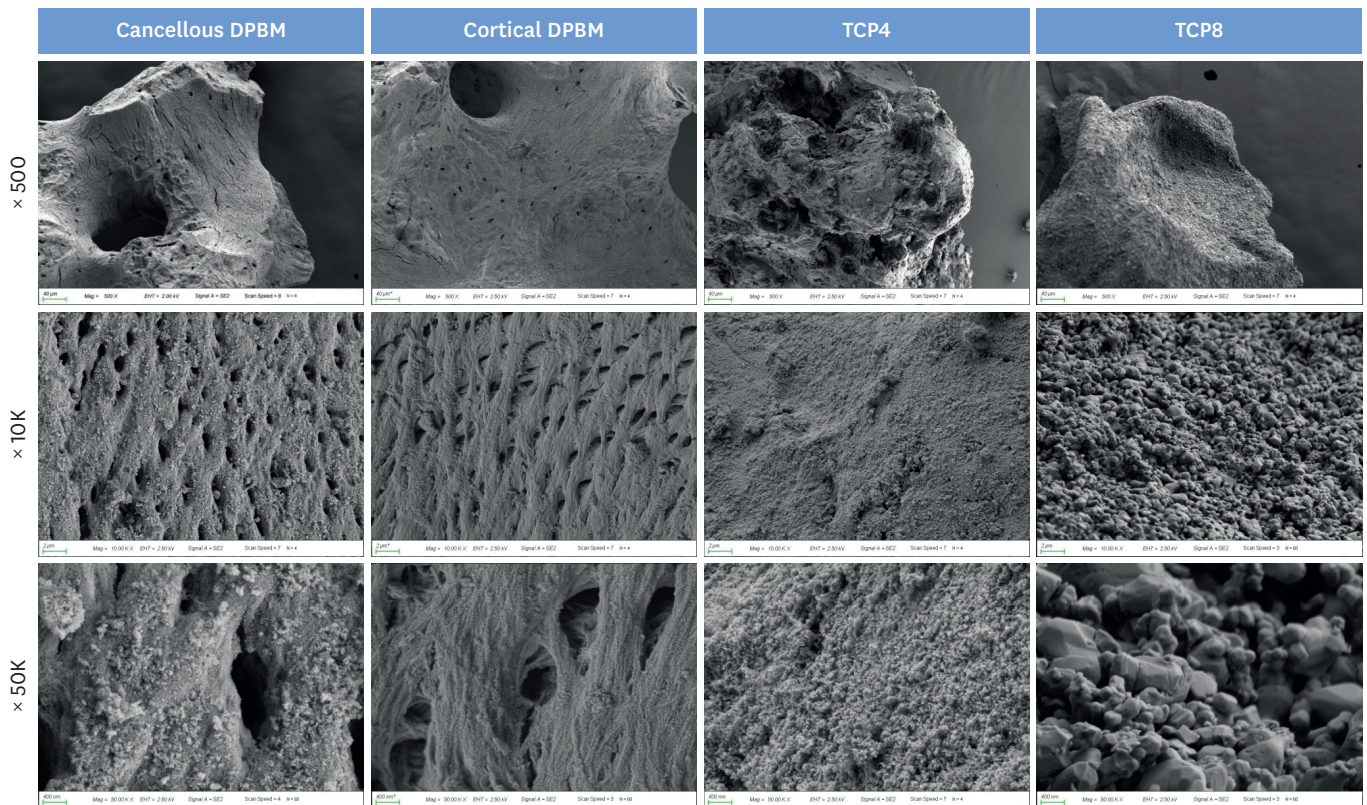


Figure 1. Scanning electron microscopy images of the bone substitutes. DPBM: deproteinized porcine bone mineral, TCP4: biphasic calcium phosphate with 6:4 ratio of hydroxyapatite:β-tricalcium phosphate, TCP8: biphasic calcium phosphate with 2:8 ratio of hydroxyapatite:β-tricalcium phosphate.

Surgical procedure

The animals were anesthetized with an intravascular injection of a mixture of Zoletil (0.1 mg/kg, Virbac, Carros, France) and Rompun (2.3 mg/kg, Bayer Korea, Ansan, Korea) by an experienced veterinarian. The surgical site was shaved and disinfected with povidone before the skin incision, followed by local anesthesia with 1:100,000 epinephrine lidocaine. An incision was made through the midline of the frontal bone. Subsequently, a full-thickness flap was elevated to expose the surgical area. Four standardized circular defects, each with a diameter of 8 mm, were created using an 8-mm-diameter trephine bur, with copious saline irrigation to prevent thermal damage to the bone. The drilling was performed in a gradual manner, with frequent pauses to assess depth and check for dural integrity (**Figure 2A and B**). Vital signs were constantly monitored throughout the procedure. Hemostasis was achieved using sterile gauze compression as needed during flap elevation. Bone graft materials with an absorbable collagen membrane were randomly assigned to the defects in the calvarium of rabbits according to the groups listed above (**Figure 2C and D**).

After treatment, the periosteum and subcutaneous tissue were repositioned and sutured using absorbable sutures (Vicryl 4-0, Ethicon, Johnson & Johnson, Somerville, NJ, USA), while the scalp was closed with absorbable sutures (Monosyn 5-0, B. Braun, Melsungen, Germany) (**Figure 2E and F**). All animals received injections of antibiotics (cefazolin, 15 mg/kg, intravenous) and analgesics (Metacam, 0.2 mg/kg, intravenous) to manage infection and pain for 3 days post-surgery. Clinical observations were conducted weekly to monitor for any abnormalities at the surgical site. The animals received care at least twice daily following treatment until they were sacrificed.

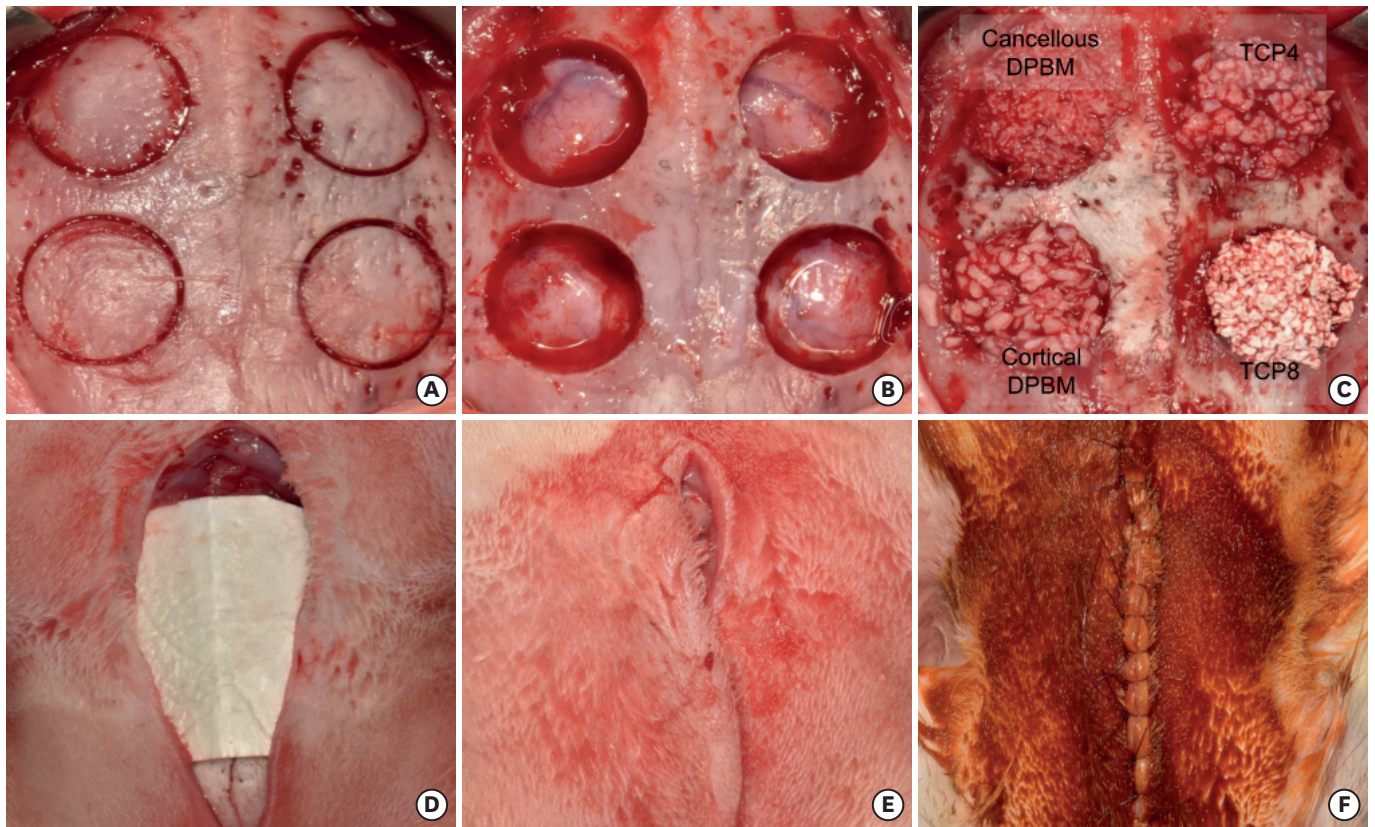


Figure 2. Clinical photographs of the experiment. (A, B) Four 8-mm-diameter defects were made in the calvaria of 12 rabbits. (C) Bone graft materials were applied to the defects. (D) A collagen membrane was used to cover the bone graft area. (E) After the bone graft, a subcutaneous suture was performed first. (F) A skin suture was performed, and the soft tissue was repositioned. DPBM: deproteinized porcine bone mineral, TCP4: biphasic calcium phosphate with a 6:4 ratio of hydroxyapatite:β-tricalcium phosphate, TCP8: biphasic calcium phosphate with a 2:8 ratio of hydroxyapatite:β-tricalcium phosphate.

Specimen preparation

Animals were euthanized at 6 and 12 weeks after surgery via an injection of potassium chloride into the carotid artery. Following euthanasia, the specimens, including the experimental sites, were collected. These harvested block sections were then dissected and fixed in 10% neutral-buffered formalin for 2 weeks. Before sectioning, the fixed block specimens underwent scanning with micro-computed tomography (micro-CT; CTAn, Bruker-CT).

Evaluation method

Radiological analysis

In micro-CT analysis, the samples were scanned with a high-resolution cone beam micro-CT device (SkyScan-1173, Skyscan, Kontich, Belgium), and the resulting files were saved as 2,240 × 2,240 pixel BMP files. The micro-CT included specific exposure conditions such as 92 kV voltage, 120 mA current, 500 ms exposure time, a rotation step of 0.3°, frame average of 4, a 1.0-mm aluminum filter and an image pixel size of 19.18 μm. Bone volume/tissue volume (BV/TV), graft/bone volume (GV/BV), and bone surface/tissue volume (BS/TV) were assessed at 6 and 12 weeks. Additionally, to evaluate bone quality, parameters such as trabecular bone pattern (Tb.Pf), trabecular thickness (Tb.Th), and trabecular number (Tb.N) were analyzed. The volume of interest was determined by the boundaries of each bone defect. The calculations for bone graft particles and newly formed bone tissue were based on 90–225 grayscale and 55–89 grayscale values, respectively (Figure 3).

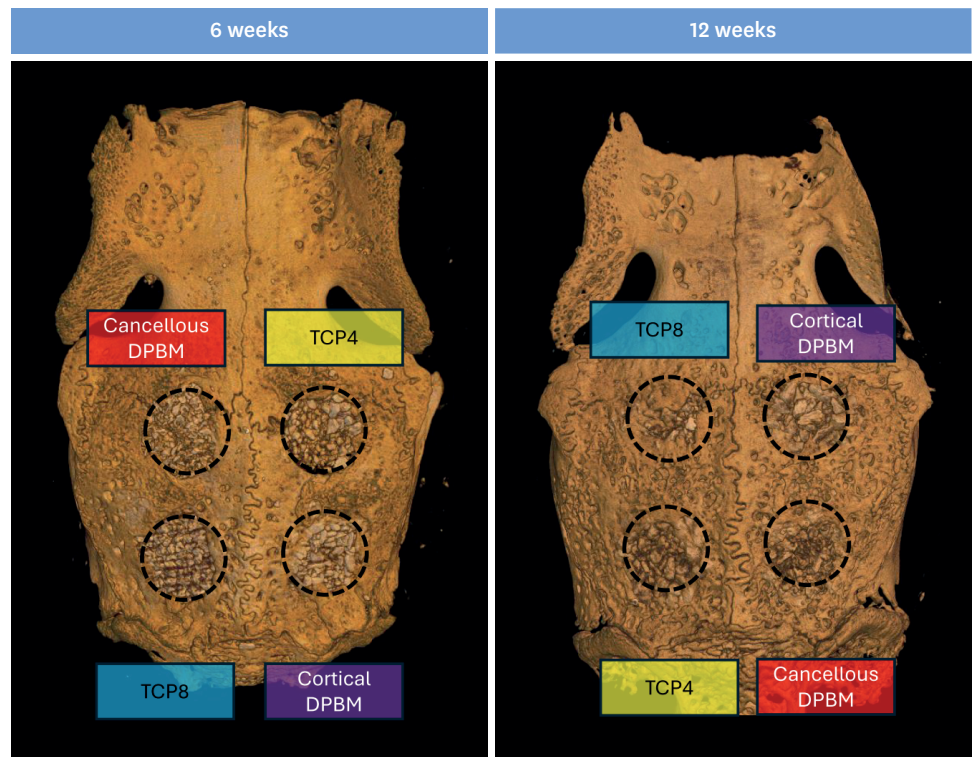


Figure 3. Axial view of the micro-computed tomography analysis at 6 weeks and 12 weeks post-surgery. DPBM: deproteinized porcine bone mineral, TCP4: biphasic calcium phosphate with a 6:4 ratio of hydroxyapatite: β -tricalcium phosphate, TCP8: biphasic calcium phosphate with a 2:8 ratio of hydroxyapatite: β -tricalcium phosphate.

Histological observation

The histological and radiographic analyses were conducted by the same experienced researcher. The fixed block specimen was sectioned into slices 6–8 μ m thick and subsequently stained with Masson's trichrome for examination under an optical microscope. Observations were made of the bone graft material and the tissue reaction in the area of the absorbable membrane.

Histometric observations

The following landmarks were measured and calculated using an image analysis program (ImageJ, National Institutes of Health, Bethesda, MD, USA).

- ① Newly formed bone area (%): newly formed bone area relative to the total augmented area.
- ② Fibrovascular connective tissue (FVCT) area (%): FVCT relative to the total augmented area.
- ③ Residual bone substitutes area (%): sum of the residual bone substitutes area relative to the total augmented area.

Statistical analysis

Outcome parameters derived from micro-CT and histomorphometric analyses were presented as median and interquartile range. The data were analyzed using the GraphPad statistical software (GraphPad Software Inc., San Diego, CA, USA), and statistically significant differences were identified through the Kruskal-Wallis test followed by Dunn's multiple comparison test ($P < 0.05$). Measurements were conducted biweekly to assess intra-examiner reliability. Histomorphometric measurements were repeated after a one-week interval. Intra-examiner reliability was evaluated using the intraclass correlation coefficient, which demonstrated high reliability with a value of 0.93.

RESULTS

Clinical findings

The histologic views at 6 and 12 weeks are shown in **Figures 4** and **5**, respectively. In all 4 groups, the augmented areas were healing uneventfully, with no signs of inflammation related to the graft materials.

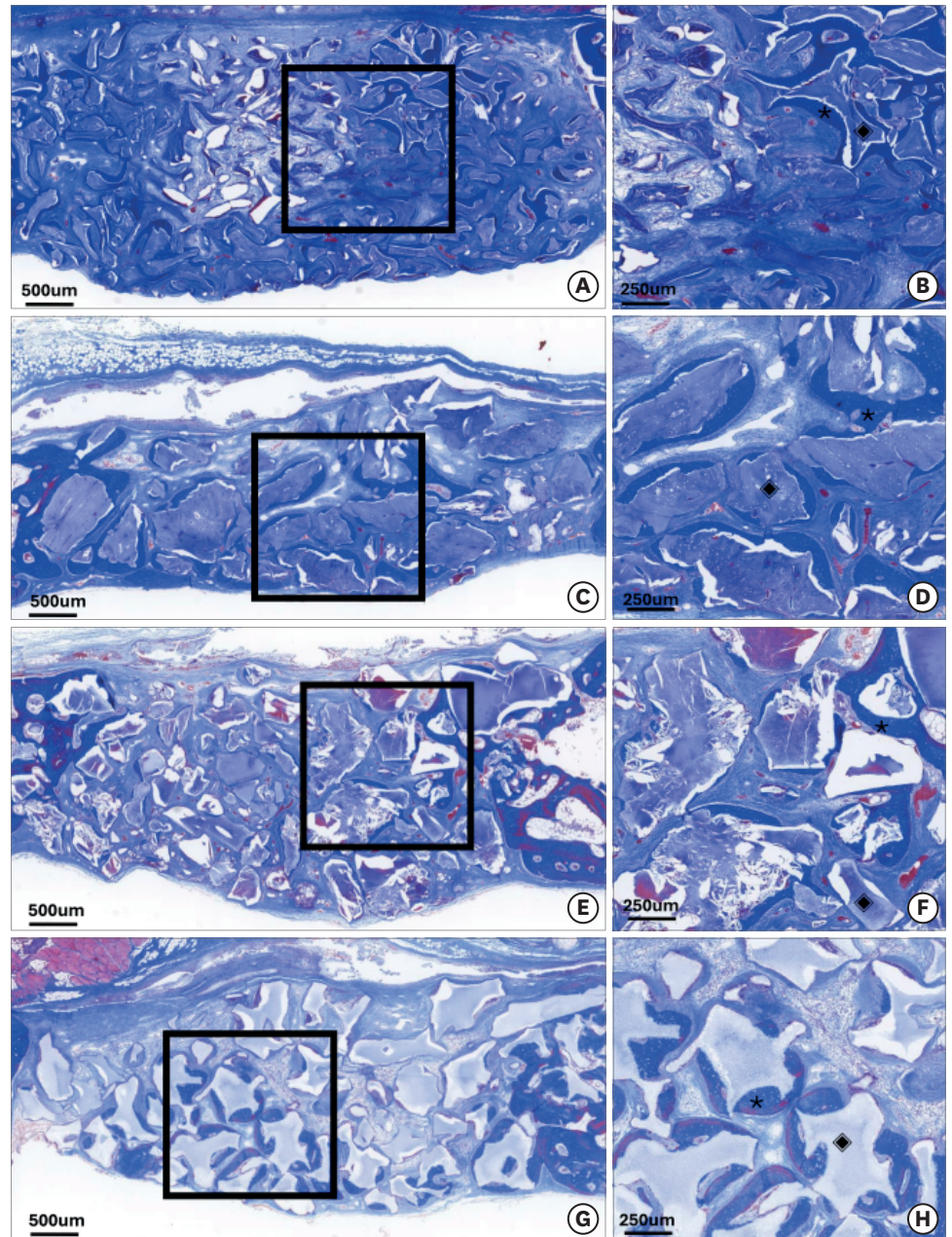


Figure 4. Histologic view of the experimental groups at 6 weeks. (A, B) Cancellous DPBM; (C, D) Cortical DPBM; (E, F) TCP4; and (G, H) TCP8. *: newly formed bone; ◆: residual bone substitutes. DPBM: deproteinized porcine bone mineral, TCP4: biphasic calcium phosphate with a 6:4 ratio of hydroxyapatite:β-tricalcium phosphate, TCP8: biphasic calcium phosphate with a 2:8 ratio of hydroxyapatite:β-tricalcium phosphate.

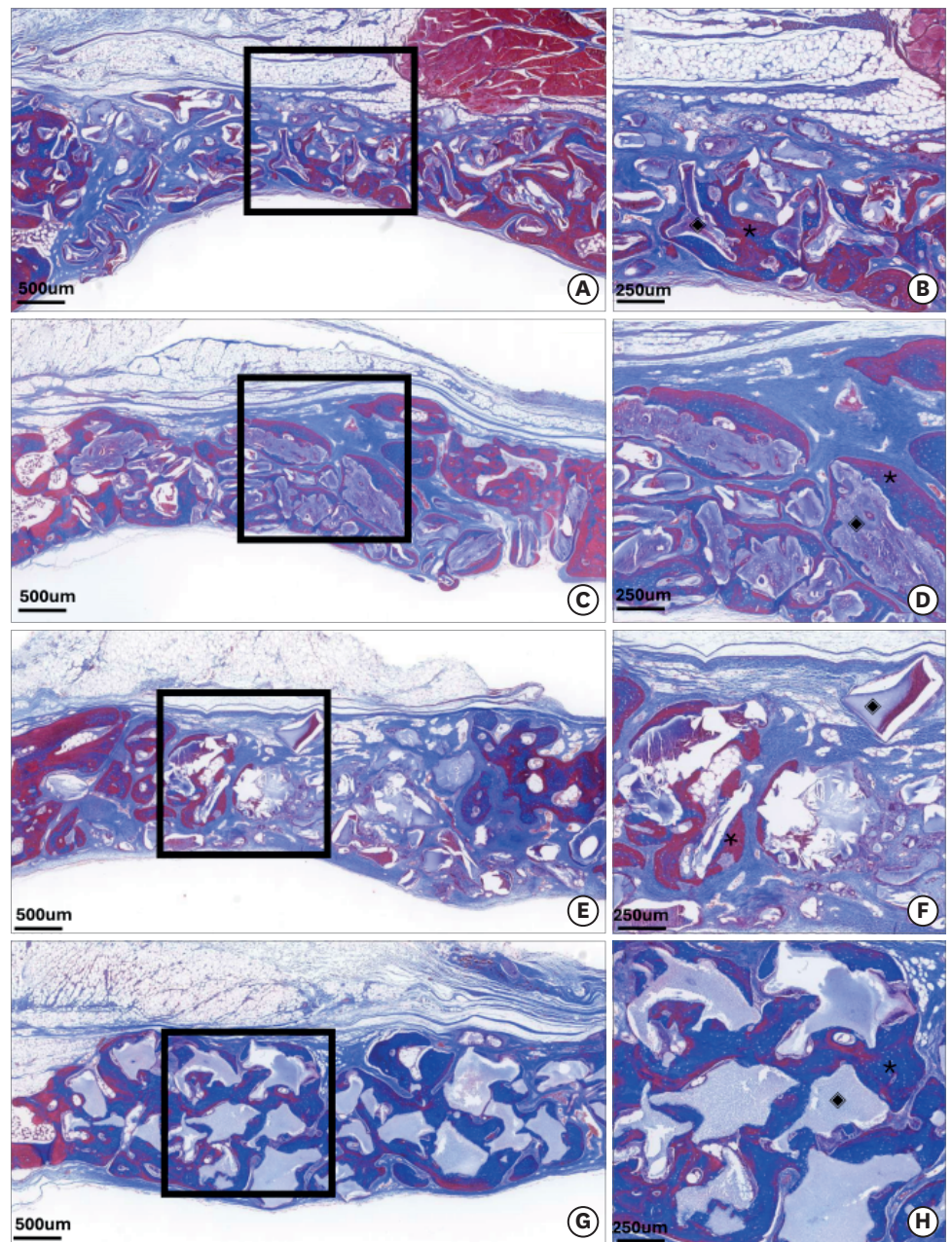


Figure 5. Histologic view of the experimental groups at 12 weeks. (A, B) Cancellous DPBM; (C, D) Cortical DPBM; (E, F) TCP4; and (G, H) TCP8. *: newly formed bone; ◆: residual bone substitutes. DPBM: deproteinized porcine bone mineral, TCP4: biphasic calcium phosphate with a 6:4 ratio of hydroxyapatite:β-tricalcium phosphate, TCP8: biphasic calcium phosphate with a 2:8 ratio of hydroxyapatite:β-tricalcium phosphate.

Micro-CT analysis

The radiographic analysis at 6 and 12 weeks is summarized in **Figure 6**.

After a 6-week observation period, no statistically significant differences were observed among the 4 experimental groups in parameters such as BV/TV ($P=0.4159$), GV/TV ($P=0.2264$), and BS/TV ($P=0.6655$). Additionally, Tb.Pf ($P=0.1684$), Tb.Th ($P=0.7900$), and Tb.N ($P=0.5346$) showed no significant differences between the groups.

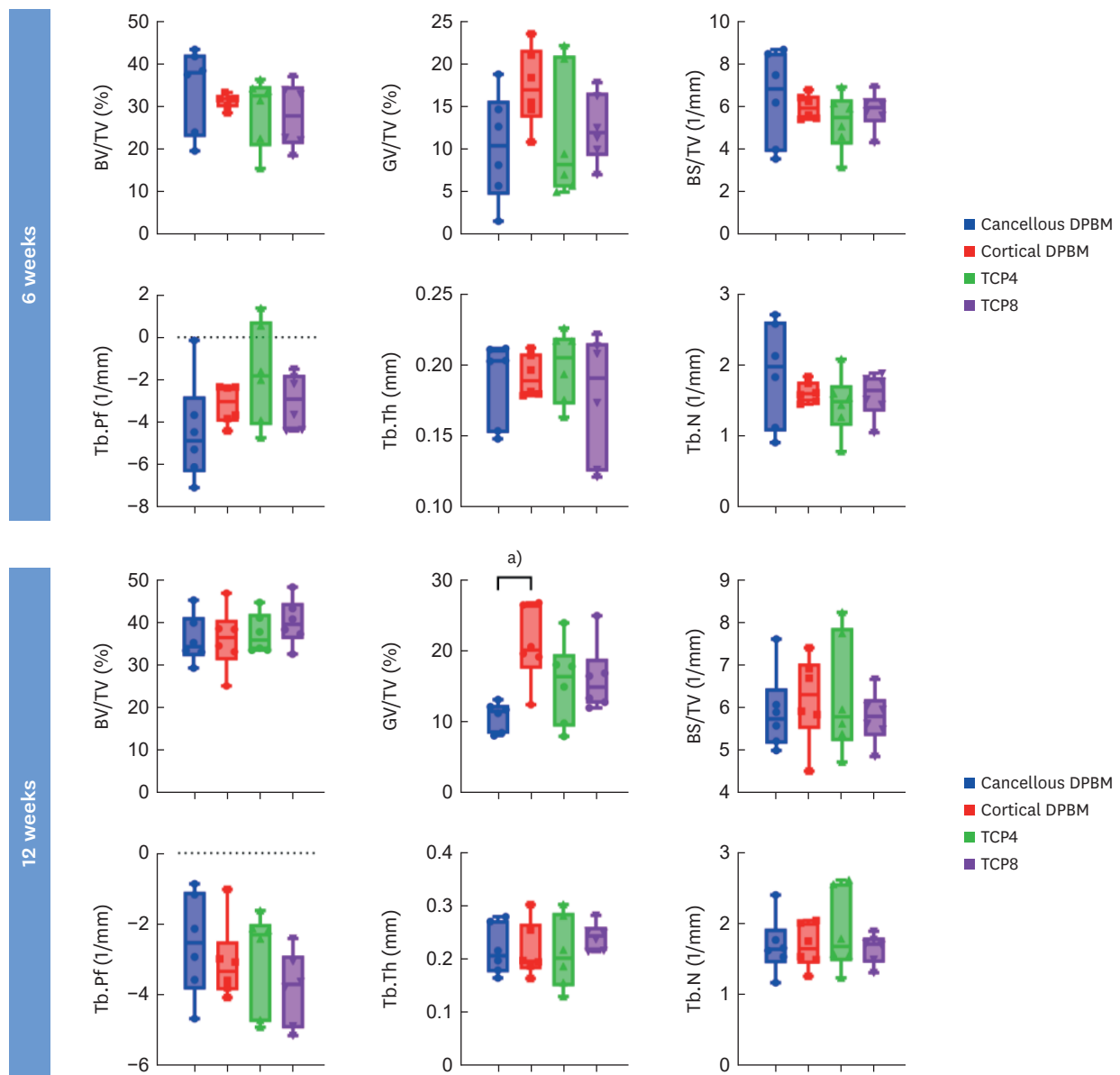


Figure 6. Results of the micro-computed tomography analysis of the experimental groups using different bone substitutes at 6 and 12 weeks, in a box and whisker plot with individual data points displayed. At 6 weeks, there was no statistically significant difference in the proportion of bone volume, graft volume and bone surface to the total volume. Additionally, Tb.pf, Tb.Th and Tb.N were comparable. At 12 weeks, however, GV/TV showed a significant difference between cancellous bone and cortical bone. No statistically significant differences were observed in other factors.

DPBM: deproteinized porcine bone mineral, TCP4: biphasic calcium phosphate with a 6:4 ratio of hydroxyapatite:β-tricalcium phosphate, TCP8: biphasic calcium phosphate with a 2:8 ratio of hydroxyapatite:β-tricalcium phosphate, BV/TV: bone volume/tissue volume, GV/TV: graft volume/tissue volume, BS/TV: bone surface/tissue volume, Tb.Pf: trabecular bone pattern, Tb.Th: trabecular thickness, Tb.N: trabecular number.

Lower case letters in superscripts indicate significant differences between groups (^a*P*<0.05).

At the 12-week observation point, no significant differences were observed in BS/BV (*P*=0.8857) and BS/TV (*P*=0.3156) across the groups. Similarly, the values for Tb.Pf, Tb.Th, and Tb.N showed no significant differences (*P*=0.3156, *P*=0.6579, and *P*=0.9040, respectively). However, a significant difference in GV/TV was noted among the groups (*P*=0.0165). Further analysis through multiple comparisons indicated that the cortical DPBM group had a significantly higher GV/TV than the cancellous DPBM group (*P*=0.0087).

Histomorphometric analysis

The histomorphometric analysis at 6 and 12 weeks is summarized in **Figure 7** and **Supplementary Tables 1** and **2**.

At the 6-week observation point, the percentage of residual bone substitute area was comparable across all groups, ranging from 11.29% to 12.27%. Variability was observed in the percentage of newly formed bone area among the groups, with the highest percentage (45.24%) in the TCP8 group and the lowest (36.16%) in the TCP4 group; however, these differences were not statistically significant. The percentage of FVCT was highest in the TCP4 group (50.00%) and lowest in the cancellous DPBM group (38.68%), though these differences were also not statistically significant.

At the 12-week observation point, notable changes were observed in all parameters except the percentage of residual bone substitute area. The cortical DPBM group recorded the highest residual bone substitute area at 15.96%, while the porcine cancellous bone group had the lowest at 5.87%, a difference that was statistically significant ($P=0.0027$). The percentage of newly formed bone area increased across all groups compared to the 6-week mark. The TCP8 group demonstrated the highest increase at 50.96%, and the porcine cancellous bone group the lowest at 42.88%, though these differences were not statistically significant. The maturation and remodeling of FVCT into mineralized tissue were evident across all groups, reflecting the bone healing process. Levels of FVCT area also varied significantly, with the porcine cancellous bone group exhibiting the highest percentage at 42.69% and the TCP8 group the lowest at 29.18%; however, these differences were not statistically significant. The inverse relationship between FVCT and the newly formed bone percentage suggests that a successful

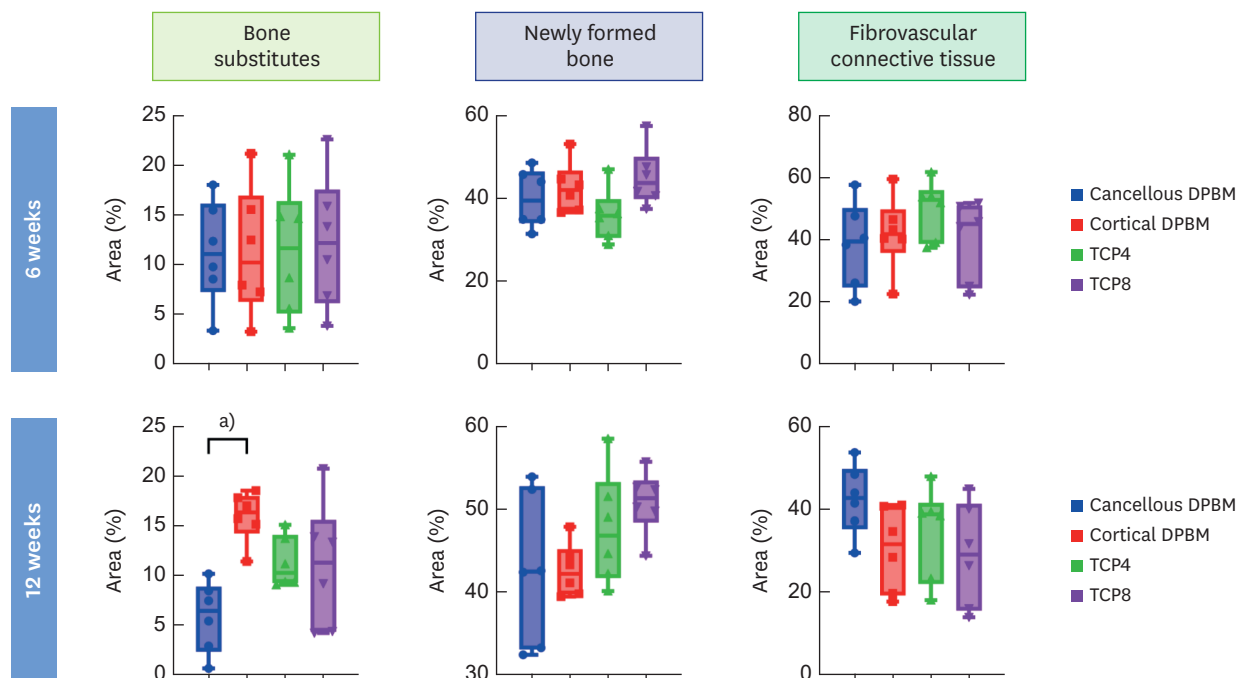


Figure 7. Results of the histomorphometric analysis of the experimental groups using different bone substitutes at 6 and 12 weeks, in a box and whisker plot with individual data points displayed.

DPBM: deproteinized porcine bone mineral, TCP4: biphasic calcium phosphate with a 6:4 ratio of hydroxyapatite:β-tricalcium phosphate, TCP8: biphasic calcium phosphate with a 2:8 ratio of hydroxyapatite:β-tricalcium phosphate.

Lower case letters in superscripts indicate significant differences between groups (^a $P<0.05$).

transition was completed from provisional matrix to mature bone tissue. Furthermore, the balance between FVCT resorption and new bone formation appeared to be material-dependent, potentially affecting the timeline of complete graft incorporation and mechanical stability.

DISCUSSION

This study aimed to analyze the bone regeneration and biosorption patterns of different bone substitutes in a rabbit skull defect model. The results showed that all tested bone substitutes, including cortical and cancellous DPBM and BCP with varying ratios of HA to β -TCP, supported bone regeneration. However, significant differences were noted in the GV/TV ratio at 12 weeks, with cortical DPBM exhibiting a higher GV/TV ratio than cancellous DPBM. This indicates that the structural characteristics of the bone substitute may affect the biosorption of bone substitutes during bone regeneration over time.

The percentage of newly formed bone area ranged from 36.16% to 45.24% at the 6-week observation point, and from 42.88% to 50.96% at 12 weeks. Although previous studies on xenografts and alloplasts in rabbit skull did not follow the same experimental design as our current study, their findings exhibited similar trends, showing an increase in new bone formation over time without any inflammation [29-31]. The findings are consistent with previous research indicating that xenografts, particularly those derived from porcine bone and/or BCP containing HA and β -TCP, can serve as effective alternatives to autografts.

The increased biosorption observed in cancellous DPBM compared to cortical DPBM at 12 weeks has significant clinical implications. The higher biosorption rate of cancellous DPBM suggests that it may be more suitable for applications requiring faster integration and turnover of the graft material. In contrast, cortical DPBM may be preferred in scenarios where prolonged structural support is necessary. These findings can assist clinicians in selecting the appropriate type of bone substitute based on the specific requirements of the surgical procedure and the desired healing timeline. The biological response of cortical DPBM and cancellous DPBM is somewhat similar to the response of HA and β -TCP in synthetic bone, respectively. Specifically, cortical DPBM and HA are less resorbable than cancellous DPBM and β -TCP [32]. Just as synthetic bone is commercialized and used as BCP, a mixture of HA and β -TCP, it is considered that cortical DPBM and cancellous DPBM can also be used in a mixed form.

This study also examined the effects of varying HA/ β -TCP ratios in BCP on bone regeneration. While the ratios of 6:4 (TCP4) and 2:8 (TCP8) demonstrated different percentages of newly formed bone area, these differences were not statistically significant. This indicates that although the HA/ β -TCP ratio may affect the initial process of bone formation, other factors, such as the biological environment and mechanical stability, play essential roles as well. The lack of significant differences between the TCP4 and TCP8 groups suggests that the HA/ β -TCP ratio may not be a critical factor for bone regeneration within the scope of this study. Indeed, previous research has shown that the HA/ β -TCP ratio does not significantly impact bone regeneration [33,34]. Although β -TCP is readily absorbed *in vivo*, the optimal HA ratio above which β -TCP remains effective is not yet established, and it is believed to have no significant influence on the overall new bone content. Additionally, future research could benefit from examining alternative HA/ β -TCP ratios and exploring combinations of bone substitutes with growth factors or stem cells, potentially uncovering some significant differences that our current research did not detect.

Interestingly, this study observed creeping substitution across all bone substitutes, with no evidence of reverse creeping substitution. This contrasts with previous findings where reverse creeping substitution was noted, typically in block-type cortical autografts [12,13]. The differences noted in this study suggest that the source of the bone substitute, as well as its size and/or form, are critical determinants in the bone healing process. Block-type cortical autografts tend to exhibit reverse creeping substitution, likely due to their larger size and low porosity, necessitating initial osteoclastic activity before osteoblastic activity can occur. The parameters of size and porosity of bone substitutes play a pivotal role in their integration and function. Smaller, particulate bone substitutes, used in this study, provide a larger surface area for cellular interactions and vascular infiltration, promoting quicker integration and remodeling. In contrast, block-type grafts, while offering initial structural support, may require longer remodeling periods due to their reduced surface area and the necessity for resorption before new bone formation can occur.

The biological mechanisms underlying bone healing with different substitutes can vary significantly. Creeping substitution, which involves the gradual resorption of the graft material and its replacement with new bone, was observed in all substitutes used in this study. This process is crucial for the successful integration of the graft and the long-term stability of the regenerated bone. Conversely, reverse creeping substitution, observed with block-type cortical autografts, involves initial resorption followed by new bone formation. This highlights the interplay between osteoclasts and osteoblasts during the healing process.

The use of a rabbit skull defect model provides a controlled environment for studying bone regeneration [17,27,35]; however, it may not fully capture the complexity of human clinical scenarios. Additionally, the relatively short observation periods (6 and 12 weeks) may not adequately reflect the long-term outcomes of bone substitute integration and resorption. Future studies with extended follow-up periods and larger sample sizes are necessary to validate these findings and to further explore the long-term performance of these materials. Further research should also investigate the molecular and cellular mechanisms that underlie the observed differences in bone regeneration and biosorption patterns. Understanding the interactions between bone substitutes and host tissue at the microscopic level could offer insights into optimizing the design and composition of bone graft materials. Additionally, exploring combination therapies, such as the incorporation of growth factors or stem cells with bone substitutes, could improve the regenerative capacity and clinical outcomes [27,36-38].

In conclusion, this study demonstrated that all tested bone substitutes support bone regeneration in a rabbit skull defect model. Cortical DPBM exhibited superior GV/TV and residual bone substitutes (%) at 12 weeks compared to cancellous DPBM. These findings underscore the importance of considering the structural characteristics and biosorption rates of bone substitutes in clinical decision-making. Although the HA/ β -TCP ratio did not show significant differences in bone formation, the results suggest that both TCP4 and TCP8 ratios are viable options for bone regeneration. Additionally, the observation of creeping substitution without reverse creeping substitution highlights the influence of the bone substitute's size and form on the healing process. It is also promising to re-examine the need for studies with longer observation periods to validate these findings in more complex models that more closely resemble human clinical situations [39, 40]. Such research can help refine the use of bone substitutes in guided bone regeneration protocols, ultimately enhancing patient outcomes in dental and orthopedic surgery.

SUPPLEMENTARY MATERIALS

Supplementary Table 1

The outcome of histomorphometric analysis at 6 weeks

Supplementary Table 2

The outcome of histomorphometric analysis at 12 weeks

REFERENCES

- Miron RJ, Hedbom E, Saulacic N, Zhang Y, Sculean A, Bosshardt DD, et al. Osteogenic potential of autogenous bone grafts harvested with four different surgical techniques. *J Dent Res* 2011;90:1428-33. [PUBMED](#) | [CROSSREF](#)
- Heimes D, Pabst A, Becker P, Hartmann A, Kloss F, Tunkel J, et al. Comparison of morbidity-related parameters between autologous and allogeneic bone grafts for alveolar ridge augmentation from patients' perspective-a questionnaire-based cohort study. *Clin Implant Dent Relat Res* 2024;26:170-82. [PUBMED](#) | [CROSSREF](#)
- Pyo SW, Kim KR, Chang JS, Kim S. Maxillary anterior implant-supported restorations with allogeneic block-bone graft: a report of two clinical cases. *J Implant Appl Sci* 2023;27:46-55. [CROSSREF](#)
- McKenna GJ, Gjengedal H, Harkin J, Holland N, Moore C, Srinivasan M. Effect of autogenous bone graft site on dental implant survival and donor site complications: a systematic review and meta-analysis. *J Evid Based Dent Pract* 2022;22:101731. [PUBMED](#) | [CROSSREF](#)
- Norton MR, Odell EW, Thompson ID, Cook RJ. Efficacy of bovine bone mineral for alveolar augmentation: a human histologic study. *Clin Oral Implants Res* 2003;14:775-83. [PUBMED](#) | [CROSSREF](#)
- Lee YJ, Lee SJ. Evaluation of linear and volumetric changes in bone grafts after sinus floor elevation using a lateral approach. *J Implant Appl Sci* 2022;26:73-83. [CROSSREF](#)
- Lai VJ, Michalek JE, Liu Q, Mealey BL. Ridge preservation following tooth extraction using bovine xenograft compared with porcine xenograft: a randomized controlled clinical trial. *J Periodontol* 2020;91:361-8. [PUBMED](#) | [CROSSREF](#)
- Lee JH, Yi GS, Lee JW, Kim DJ. Physicochemical characterization of porcine bone-derived grafting material and comparison with bovine xenografts for dental applications. *J Periodontal Implant Sci* 2017;47:388-401. [PUBMED](#) | [CROSSREF](#)
- Lee JH, Han JH, Jeong SN. Porcine-derived soft block bone substitutes for the treatment of severe class II furcation-involved mandibular molars: a prospective controlled follow-up study. *J Periodontal Implant Sci* 2023;53:406-16. [PUBMED](#) | [CROSSREF](#)
- Hölzer A, Pietschmann MF, Rösl C, Hentschel M, Betz O, Matsuura M, et al. The interrelation of trabecular microstructural parameters of the greater tubercle measured for different species. *J Orthop Res* 2012;30:429-34. [PUBMED](#) | [CROSSREF](#)
- Bracey DN, Seyler TM, Jinnah AH, Lively MO, Willey JS, Smith TL, et al. A decellularized porcine xenograft-derived bone scaffold for clinical use as a bone graft substitute: a critical evaluation of processing and structure. *J Funct Biomater* 2018;9:45. [PUBMED](#) | [CROSSREF](#)
- Goldberg VM, Stevenson S. Natural history of autografts and allografts. *Clin Orthop Relat Res* 1987:7-16. [PUBMED](#)
- Burchardt H. The biology of bone graft repair. *Clin Orthop Relat Res* 1983:28-42. [PUBMED](#)
- Cypher TJ, Grossman JP. Biological principles of bone graft healing. *J Foot Ankle Surg* 1996;35:413-7. [PUBMED](#) | [CROSSREF](#)
- Lee JH, An HW, Im JS, Kim WJ, Lee DW, Yun JH. Evaluation of the clinical and radiographic effectiveness of treating peri-implant bone defects with a new biphasic calcium phosphate bone graft: a prospective, multicenter randomized controlled trial. *J Periodontal Implant Sci* 2023;53:306-17. [PUBMED](#) | [CROSSREF](#)
- Park JB, Kim I, Lee W, Kim H. Evaluation of the regenerative capacity of stem cells combined with bone graft material and collagen matrix using a rabbit calvarial defect model. *J Periodontal Implant Sci* 2023;53:467-77. [PUBMED](#) | [CROSSREF](#)
- Lim HC, Paeng KW, Jung UW, Benic GI. Vertical bone augmentation using collagenated or non-collagenated bone substitute materials with or without recombinant human bone morphogenetic protein-2 in a rabbit calvarial model. *J Periodontal Implant Sci* 2023;53:429-43. [PUBMED](#) | [CROSSREF](#)

18. Lin L, Chow KL, Leng Y. Study of hydroxyapatite osteoinductivity with an osteogenic differentiation of mesenchymal stem cells. *J Biomed Mater Res A* 2009;89A:326-35. [PUBMED](#) | [CROSSREF](#)
19. Ambard AJ, Mueninghoff L. Calcium phosphate cement: review of mechanical and biological properties. *J Prosthodont* 2006;15:321-8. [PUBMED](#) | [CROSSREF](#)
20. Lambert F, Léonard A, Drion P, Sourice S, Layrolle P, Rompen E. Influence of space-filling materials in subantral bone augmentation: blood clot vs. autogenous bone chips vs. bovine hydroxyapatite. *Clin Oral Implants Res* 2011;22:538-45. [PUBMED](#) | [CROSSREF](#)
21. Jensen SS, Broggin N, Hjørting-Hansen E, Schenk R, Buser D. Bone healing and graft resorption of autograft, anorganic bovine bone and beta-tricalcium phosphate. A histologic and histomorphometric study in the mandibles of minipigs. *Clin Oral Implants Res* 2006;17:237-43. [PUBMED](#) | [CROSSREF](#)
22. Nery EB, LeGeros RZ, Lynch KL, Lee K. Tissue response to biphasic calcium phosphate ceramic with different ratios of HA/beta TCP in periodontal osseous defects. *J Periodontol* 1992;63:729-35. [PUBMED](#) | [CROSSREF](#)
23. Lee J, Lee YM, Lim YJ, Kim B. Ridge augmentation using beta-tricalcium phosphate and biphasic calcium phosphate sphere with collagen membrane in chronic pathologic extraction sockets with dehiscence defect: a pilot study in beagle dogs. *Materials (Basel)* 2020;13:1452. [PUBMED](#) | [CROSSREF](#)
24. Arunjaroenusuk S, Panmekiate S, Pimkhaokham A. The stability of augmented bone between two different membranes used for guided bone regeneration simultaneous with dental implant placement in the esthetic zone. *Int J Oral Maxillofac Implants* 2018;33:206-16. [PUBMED](#) | [CROSSREF](#)
25. Arinze TL, Tran T, Mcalary J, Daculsi G. A comparative study of biphasic calcium phosphate ceramics for human mesenchymal stem-cell-induced bone formation. *Biomaterials* 2005;26:3631-8. [PUBMED](#) | [CROSSREF](#)
26. De Risi V, Clementini M, Vittorini G, Mannocci A, De Sanctis M. Alveolar ridge preservation techniques: a systematic review and meta-analysis of histological and histomorphometrical data. *Clin Oral Implants Res* 2015;26:50-68. [PUBMED](#) | [CROSSREF](#)
27. Yun J, Lee J, Ha CW, Park SJ, Kim S, Koo KT, et al. The effect of 3-D printed polylactic acid scaffold with and without hyaluronic acid on bone regeneration. *J Periodontol* 2022;93:1072-82. [PUBMED](#) | [CROSSREF](#)
28. Yun J, Lee J, Kim S, Koo KT, Seol YJ, Lee YM. The effect of hard-type crosslinked hyaluronic acid with particulate bone substitute on bone regeneration: positive or negative? *J Periodontal Implant Sci* 2022;52:312-24. [PUBMED](#) | [CROSSREF](#)
29. Saulacic N, Fujioka-Kobayashi M, Kimura Y, Bracher AI, Zihlmann C, Lang NP. The effect of synthetic bone graft substitutes on bone formation in rabbit calvarial defects. *J Mater Sci Mater Med* 2021;32:14. [PUBMED](#) | [CROSSREF](#)
30. Park JW, Kim ES, Jang JH, Suh JY, Park KB, Hanawa T. Healing of rabbit calvarial bone defects using biphasic calcium phosphate ceramics made of submicron-sized grains with a hierarchical pore structure. *Clin Oral Implants Res* 2010;21:268-76. [PUBMED](#) | [CROSSREF](#)
31. Hong I, Khalid AW, Pae HC, Cha JK, Lee JS, Paik JW, et al. Distinctive bone regeneration of calvarial defects using biphasic calcium phosphate supplemented ultraviolet-crosslinked collagen membrane. *J Periodontal Implant Sci* 2020;50:14-27. [PUBMED](#) | [CROSSREF](#)
32. Onodera J, Kondo E, Omizu N, Ueda D, Yagi T, Yasuda K. Beta-tricalcium phosphate shows superior absorption rate and osteoconductivity compared to hydroxyapatite in open-wedge high tibial osteotomy. *Knee Surg Sports Traumatol Arthrosc* 2014;22:2763-70. [PUBMED](#) | [CROSSREF](#)
33. Lim HC, Zhang ML, Lee JS, Jung UW, Choi SH. Effect of different hydroxyapatite:β-tricalcium phosphate ratios on the osteoconductivity of biphasic calcium phosphate in the rabbit sinus model. *Int J Oral Maxillofac Implants* 2015;30:65-72. [PUBMED](#) | [CROSSREF](#)
34. Park JC, Lim HC, Sohn JY, Yun JH, Jung UW, Kim CS. Bone regeneration capacity of two different macroporous biphasic calcium materials in rabbit calvarial defect. *J Korean Acad Periodontol* 2009;39:223-30. [CROSSREF](#)
35. Lee DN, Park JY, Seo YW, Jin X, Hong J, Bhattacharyya A, et al. Photo-crosslinked gelatin methacryloyl hydrogel strengthened with calcium phosphate-based nanoparticles for early healing of rabbit calvarial defects. *J Periodontal Implant Sci* 2023;53:321-35. [PUBMED](#) | [CROSSREF](#)
36. Li L, Lee J, Cho YD, Kim S, Seol YJ, Lee YM, et al. The optimal dosage of hyaluronic acid for bone regeneration in rat calvarial defects. *J Periodontal Implant Sci* 2023;53:259-68. [PUBMED](#) | [CROSSREF](#)
37. Lee J, Yun J, Kim KH, Koo KT, Seol YJ, Lee YM. Periodontal regeneration using recombinant human bone morphogenetic protein-2 and a bilayer collagen matrix. *J Craniofac Surg* 2020;31:1602-7. [PUBMED](#) | [CROSSREF](#)
38. Kim SH, Kim KH, Seo BM, Koo KT, Kim TI, Seol YJ, et al. Alveolar bone regeneration by transplantation of periodontal ligament stem cells and bone marrow stem cells in a canine peri-implant defect model: a pilot study. *J Periodontol* 2009;80:1815-23. [PUBMED](#) | [CROSSREF](#)

39. Ko YC, Lee J, Lee D, Seol YJ, Koo KT, Lee YM. Progression of experimental peri-implantitis in guided bone regeneration and pristine bone: a preclinical *in vivo* study. J Periodontol 2023;94:1032-44. [PUBMED](#) | [CROSSREF](#)
40. Lee D, Ko YC, Koo KT, Seol YJ, Lee YM, Lee J. A flexible membrane may improve bone regeneration by increasing hydrophilicity and conformability in lateral bone augmentation. Biomater Res 2024;28:0113. [PUBMED](#) | [CROSSREF](#)